

PL-TR-93-2089

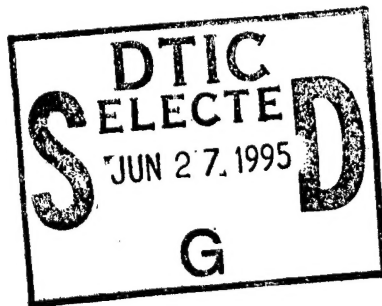
**FOUR WAVELENGTH LIDAR REMOTE SENSING
OF ATMOSPHERIC OPTICAL PROPERTIES
DURING ADVERSE WEATHER CONDITIONS**

**John M. Livingston
Edward E. Uthe**

**SRI International
333 Ravenswood Avenue
Menlo Park, CA 94025**

July 1992

**Final Report
16 March 1990-16 June 1992**



**PHILLIPS LABORATORY
Directorate of Geophysics
AIR FORCE MATERIEL COMMAND
HANSCOM AFB, MA 01731-3010**

[DTIC QUALITY INSPECTED 3]

19950626 065

"This technical report has been reviewed and is approved for publication"

Vernon D. Turner
VERNON D. TURNER
Contract Manager

Donald E. Bedo
DONALD E. BEDO, Chief
Electro-Optical Environment Br

Roger A. Van Tasel
ROGER A. VAN TASSEL, Director
Optical Environment Division

This report has been reviewed by the ESC Public Affairs Office (PA) and is releasable to the National Technical Information Service (NTIS).

Qualified requestors may obtain additional copies from the Defense Technical Information Center. All others should apply to the National Technical Information Service.

If your address has changed, or if you wish to be removed from the mailing list, or if the addressee is no longer employed by your organization, please notify PL/IM , Hanscom AFB MA 01731-3010. This will assist us in maintaining a current mailing list.

Do not return copies of this report unless contractual obligations or notices on a specific document require that it be returned.

REPORT DOCUMENTATION PAGE

*Form Approved
OMB No. 0704-0188*

Public reporting burden for this collection of information is estimated to average 1 hour per response, including the time for reviewing instructions, searching existing data sources, gathering and maintaining the data needed, and completing and reviewing the collection of information. Send comments regarding this burden estimate or any other aspect of this collection of information, including suggestions for reducing this burden, to Washington Headquarters Services, Directorate for Information Operations and Reports, 1215 Jefferson Davis Highway, Suite 1204, Arlington, VA 22202-4302, and to the Office of Management and Budget, Paperwork Reduction Project (0704-0188), Washington, DC 20503.

1. AGENCY USE ONLY (<i>Leave Blank</i>)			2. REPORT DATE July 1992	3. REPORT TYPE AND DATES COVERED Final: 16 Mar 1990—16 Jun 1992	
4. TITLE AND SUBTITLE Four-Wavelength Lidar Remote Sensing of Atmospheric Optical Properties During Adverse Weather Conditions			5. FUNDING NUMBERS Contract F19628-90-K-0027 PE 63790D PR SAF1 TA 01 WU AA		
6. AUTHOR(S) John M. Livingston Edward E. Uthe					
7. PERFORMING ORGANIZATION NAME(S) AND ADDRESS(ES) SRI International 333 Ravenswood Avenue Menlo Park, CA 94025			8. PERFORMING ORGANIZATION REPORT NUMBER Final Report SRI Project 8875		
9. SPONSORING/MONITORING AGENCY NAME(S) AND ADDRESS(ES) Phillips Laboratory 29 Randolph Road Hanscom AFB, MA 01731-3010			10. SPONSORING/MONITORING AGENCY REPORT NUMBER PL-TR-93-2089		
11. SUPPLEMENTARY NOTES					
12a. DISTRIBUTION/AVAILABILITY STATEMENT Approved for public release; distribution unlimited			12b. DISTRIBUTION CODE		
13. ABSTRACT (<i>Maximum 200 words</i>) SRI International operated a van-mounted four-wavelength lidar system during the July 1990 FLAPIR field experiment. Measurements of range-resolved relative backscatter signatures were obtained at wavelengths 0.53, 1.06, 3.8, and 10.6 μm. Backscattered signals from a passive reflecting target located 928 m from the SRI lidar van were used to estimate path-length transmission values at wavelengths 0.53, 3.8, and 10.6 μm during selected time periods. Lidar data files were transferred to a MicroVax computer and copied to a single optical disk medium that was provided to Phillips Laboratory (GP). At the request of Phillips Laboratory, an identical copy was also sent to Dr. Luc Bissonnette of Defense Research Establishment Valcartier for subsequent data analysis.					
14. SUBJECT TERMS Lidar Remote sensing Optical properties			15. NUMBER OF PAGES 24		
			16. PRICE CODE		
17. SECURITY CLASSIFICATION OF REPORT Unclassified	18. SECURITY CLASSIFICATION OF THIS PAGE Unclassified	19. SECURITY CLASSIFICATION OF ABSTRACT Unclassified	20. LIMITATION OF ABSTRACT SAR		

CONTENTS

1. BACKGROUND AND PROJECT OBJECTIVES	1
2. SRI FOUR-WAVELENGTH LIDAR SYSTEM.....	2
3. FIELD TEST AND DATA COLLECTION.....	3
4. DATA REDUCTION AND ANALYSIS.....	4
A. Data Storage and Transmittal.....	4
B. Target Identification and Detectability	4
C. Characterization of Receiver.....	4
D. Target-Derived Path-Length Transmission Values.....	5
E. Range-Resolved Backscatter Returns	13
5. DISCUSSION AND RECOMMENDATIONS	18
6. ADMINISTRATIVE INFORMATION	20
A. Contributors	20
B. Related Efforts	20

Accession For	
NTIS	CRA&I
DTIC	TAB
Unannounced	
Justification _____	
By _____	
Distribution / _____	
Availability Codes	
Dist	Avail and / or Special
A-1	

ILLUSTRATIONS

1	Example of an A-Scope Display	5
2	Graphic Depiction of Table 1 Data	10
3	Mean Lidar Target Return Measurements and Least-Squares Fits for 21 July 1990	12
4	Target-Derived Transmission Percentages for 2244–2322 EDT, 27 July 1990 ...	13
5	Lidar Range-Resolved Relative Backscatter Signatures for 0647:18 EDT, 21 July 1990	14
6	Lidar Range-Resolved Relative Backscatter Signatures for 0219:26 EDT, 19 July 1990	16
7	Lidar Range-Resolved Relative Backscatter Signatures for 0259:41 EDT, 16 July 1990, After Range-Squared Correction	17

TABLES

1	Times of Lidar Data Acquisition and Target Detection for 16 July and 19-27 July.....	6
2	SRI FLAPIR Four-Wavelength Lidar Calibration Results	12

1. BACKGROUND AND PROJECT OBJECTIVES

During a two-week period in July 1990, the United States Air Force Phillips Laboratory (GP) conducted an intensive field experiment using a variety of optical sensors at the Brunswick, Maine, Naval Air Station. This trial was named FLAPIR (an acronym for FLIR* and lidar atmospheric propagation in the infrared). The objective of the FLAPIR program is to determine whether information obtained from lidar measurements can be used to predict the performance of a forward-looking infrared (FLIR) electrooptical system during adverse weather conditions. In support of Phillips Laboratory, SRI International operated its four-wavelength lidar system during the FLAPIR field tests. The primary role of SRI's participation was to operate the lidar system and to provide Phillips Laboratory with the lidar backscatter data obtained during the trial. SRI was also to assist Phillips Laboratory in the analysis of those data by calculating path transmission values for comparison with the dual-wavelength infrared (DUWIR) camera measurements.

*An acronym for forward-looking infrared.

2. SRI FOUR-WAVELENGTH LIDAR SYSTEM

Under funding from the Army Research Office, SRI developed a four-wavelength lidar system to investigate multiple-wavelength lidar techniques for quantitative aerosol property measurements from remote distances. The system is also effective for evaluating propagation effects at wavelengths commonly used by DoD laser systems. The SRI system, which is installed in a 20-ft van, transmits laser pulses at four wavelengths: 0.53 and 1.06 μm using an Nd laser, 3.8 μm using a DF laser, and 10.6- μm using a CO₂ laser. An optical arrangement provides for transmitting the pulses along the same horizontal path, coaxial with a common 12-inch-diameter Newtonian receiver. Wavelength-separation optics direct received energy to separate detectors for 0.53- μm , 1.06- μm , and 3.8/10.6- μm wavelength energy. A receiver multiplex circuit routes the detected 0.53- μm backscatter signature to a transient recorder on the first Nd laser firing, and the 1.06- μm backscatter signature on the second Nd laser firing. A double-pulse mode provides both firings within a 50- μs period. The multiplex unit then switches to the 3.8/10.6- μm receiver and the DF laser is pulsed about 15 μs later followed by the CO₂ laser firing at another 15- μs interval.

The transient recorder is controlled by an interrupt circuit that terminates the digitization of each firing. This arrangement provides for storage of a four-wavelength backscatter signature within the transient recorder within a 80- μs interval. The logarithmic backscatter values are then transferred to an LSI-11/24 microcomputer and written on nine-track magnetic tape, together with date and time information.

3. FIELD TEST AND DATA COLLECTION

During the FLAPIR field trial, the SRI four-wavelength lidar van was positioned alongside other instrumentation vans at the Brunswick Naval Air Station site. A passive target was placed at a distance of 928 m from the lidar van to provide for lidar sighting, calibration, eye-safety, and target returns useful for data analysis. The lidar was operated during assigned time periods between 13 July and 27 July 1990. The data-acquisition periods on 13 July served as a system shakedown. Data at each wavelength were digitized at a sampling interval of 20 ns with a precision of eight bits, and all data were recorded on nine-track magnetic tape. A real-time color graphics display was used to evaluate data quality and prevailing atmospheric scattering properties at each wavelength. No major equipment problems occurred during the period 16 July through 27 July, although several computer failures resulted in short data gaps.

4. DATA REDUCTION AND ANALYSIS

A. DATA STORAGE AND TRANSMITTAL

At the time of data acquisition, the lidar backscatter signatures at the four wavelengths were recorded together with time and date information on nine-track magnetic tape as a single fixed-length record of 8256 eight-bit bytes for each record. The actual backscatter data were stored in the last 8192 bytes (4096 16-bit words). These data were subsequently copied to a MicroVAX computer, where they are stored on optical disk as unformatted direct access files (in VAX/VMS Files-11 format) containing fixed-length (8256-byte) records, with a separate file for each physical raw data tape. Each data tape could hold up to 1200 lidar records; thus, the maximum number of records per file is 1200, although the actual number varies.

An optical disk containing the raw lidar data files in VAX/VMS Files-11 format has been sent to Lt. Col. George G. Koenig at Phillips Laboratory. This disk contains all data from 16 July through 27 July. Data collected on 13 July were excluded because no DUWIR data were taken on this day. A simple FORTRAN computer program for reading the data files was included on the disk, and written instructions were provided. At Col. Koenig's request, a duplicate disk was sent to Dr. Luc Bissonnette of Defense Research Establishment Valcartier.

B. TARGET IDENTIFICATION AND DETECTABILITY

The first data-reduction task was to examine each file and to identify when the passive reflective target was/was not detectable at each wavelength. This multiple-step procedure was described in detail in the first SRI Quarterly R&D Status Report (15 October 1990). Basically, the procedure required graphic display of numerous relative backscatter signatures, and it combined subjective analysis with an objective search routine to identify the presence or absence of a backscattered return from the target. Figure 1 is an example of a single data record that contains the backscatter signatures at each of the four wavelengths. Table 1 presents a complete listing of the times of lidar data acquisition and the times of target detection for 16 July and 19 through 27 July. Figure 2 displays graphically the information listed in Table 1. (All of these exhibits are reproduced from the first Status Report.)

C. CHARACTERIZATION OF RECEIVER LOGARITHMIC AMPLIFIER RESPONSE

A second task was to characterize the response of the logarithmic amplifiers that were used in the lidar system. This information is necessary for analyses of relative backscatter signatures, including proper removal of the geometric range dependence. During the field tests, neutral-density filters of known attenuation (nominally 3, 10, 20, and 30 dB) were inserted periodically

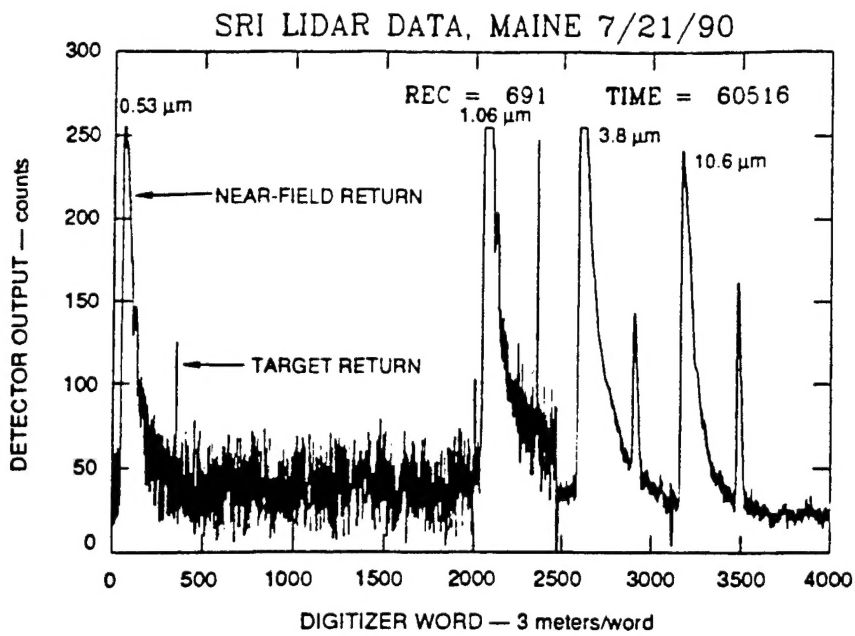


FIGURE 1 EXAMPLE OF AN A-SCOPE DISPLAY

in front of the lidar receiver(s) before recording data for a number of lidar shots. For each wavelength, the mean maximum backscattered returns (in counts) from the target were then plotted as function of filter attenuation (in dB). Linear least-squares methodology was used to derive the optimum slope (counts/dB) of each curve. Figure 3 shows the data and the results of the least-squares fit for a calibration performed on 21 July. The points represent the mean measured values, and the lines represent the regression fits, where saturated (255 counts) or nearly saturated target return data have been excluded from the regression analysis. Table 2 lists the results of the analyses of the various calibration runs. In particular, Table 2 lists the mean and one standard deviation counts-to-decibel conversion factors from series of calibration runs that apply to particular data files. The identification data file numbers to which the table values apply and the files containing the calibration runs used in calculating the values are also listed. These factors are to be used in converting the digitized signals in counts to relative decibel values.

D. TARGET-DERIVED PATH-LENGTH TRANSMISSION VALUES

Lidar signals backscattered from the reflective target positioned 928 m from the SRI transmitter/receiver were analyzed to calculate path-length transmission values at 0.53, 3.8, and 10.6 μm for selected time periods during the FLAPIR program. Hard-copy and digital output of these transmission histories were forwarded to Col. Koenig for subsequent comparison with measurements from other instruments. Data were transmitted via electronic mail. As an example, Figure 4 shows the transmission history for the period 2244 -2322 EDT on 27 July.

Table 1

TIMES OF LIDAR DATA ACQUISITION AND TARGET DETECTION FOR 16 JULY AND 19-27 JULY

Date	Tape No.	Lidar Operation Times (EDT)	Times of Target Detection		
			0.53 μm	1.06 μm	3.8 μm
16 July	6	02:33:29 - 02:48 :32	all	all	02:33:41 - end
	7	02:55:42 - 03:34:51	all	all	all
	8	03:37:45 - 03:53:45	all	all	all
	9	04:08:32 - 04:23:24	04:08:42 - end	04:08:42 - end	04:08:38 - end
	10	04:30:55 - 04:43:49	all	all	all
	11	04:51:30 - 05:09:56	beg - 05:09:56	beg - 05:09:56	beg - 05:09:56
	12	05:27:42 - 05:49:12	none	none	none
	13	05:51:24 - 06:31:02	none	none	06:19:34 - end
	14	06:32:58 - 06:47:30	none	06:33:08 - 06:35:32*	all
	15	06:54:08 - 07:07:45	07:05:47 - end	07:04:03 - end	07:01:40 - end
19 July	16	07:09:10 - 07:25:23	all	all	all
	17	02:08:28 - 02:48:24	02:08:38 - end	02:08:38 - end	02:08:34 - end
	18	02:50:02 - 02:57:04	all	all	all
	19	04:33:56 - 05:06:50	04:34:04 - end	04:34:04 - end	04:34:02 - end
	20	05:08:28 - 05:48:26	all	all	05:08:28 - 05:20:08
27 July	21	05:51:08 - 06:21:52	all	all	05:20:10 - 05:28:52*
	22	06:41:34 - 06:50:46	06:41:46 - end	06:41:46 - end	05:28:54 - end
28 July	23	06:41:46 - end	06:41:46 - end	06:41:40 - end	06:41:42 - end
	24				

Note: Frequency of target detection exceeded 95% for the time periods listed, except for those times marked by an asterisk (*), where the frequency was between 75% and 95%, or by double asterisks (**), where the frequency was less than 20%.

Table 1 (Continued)

TIMES OF LIDAR DATA ACQUISITION AND TARGET DETECTION FOR 16 JULY AND 19-27 JULY

Date	Tape No.	Lidar Operation Times (EDT)	Times of Target Detection		
			0.53 μm	1.06 μm	3.8 μm
20 July	19	06:52:56 - 07:32:54	all	all	all
	20	07:36:46 - 07:47:48	all	all	all
	21	15:22:57 - 15:34:27	15:25:01 - end	15:24:59 - end	15:24:55 - end
		15:41:46 - 16:12:00	15:41:52 - end	15:41:50 - end	15:41:50 - end
	22	16:13:36 - 16:53:34	all	all	all
	23	17:11:47 - 17:51:45	17:11:57 - end	17:11:57 - end	17:11:53 - end
21 July	24	03:36:00 - 04:15:56	none	none	none
	25	04:18:06 - 04:58:04	none	none	none
	26	05:00:36 - 05:40:34	none	none	none
	27	05:42:16 - 06:22:14	05:59:06 - end	05:58:46 - end	05:57:00 - 05:58:20*
	28	06:24:00 - 06:57:23	all	all	05:58:22 - end
	29	22:11:32 - 22:56:01	22:22:13 - end	22:22:11 - end	22:22:07 - end
22 July	30	02:46:03 - 02:51:59	02:46:11 - end	02:46:11 - end	02:46:07 - end
		02:54:07 - 03:34:05	all	all	all
					10.6 μm

Note: Frequency of target detection exceeded 95% for the time periods listed, except for those times marked by an asterisk (*), where the frequency was between 75% and 95%, or by double asterisks (**), where the frequency was less than 20%.

TIMES OF LIDAR DATA ACQUISITION AND TARGET DETECTION FOR 16 JULY AND 19-27 JULY

Date	Tape No.	Lidar Operation Times (EDT)	Times of Target Detection			
			0.53 μm	1.06 μm	3.8 μm	10.6 μm
24 July	31	03:36:03 - 04:02:59 04:21:08 - 04:34:08	all 04:21:18 - end	all 04:21:16 - end	all 04:21:12 - end	all 04:21:14 - end
	32	04:36:00 - 05:15:59	all	all	all	all
	33	15:19:56 - 15:59:52	15:20:04 - end	15:20:04 - end	15:20:00 - end	15:20:02 - end
	34	17:11:45 - 17:51:42	17:11:55 - end	17:11:53 - end	17:11:44 - end	17:11:51 - end
	35	17:53:34 - 18:28:26	all	all	all	all
	36	04:15:43 - 05:02:40	04:15:09 - end	04:15:09 - end	04:15:05 - end	04:15:05 - end
	37	05:04:30 - 05:16:33	all	all	all	all
	38	05:29:27 - 05:57:19 06:00:05 - 06:40:03	05:29:33 - end all	05:29:33 - end all	05:29:29 - end all	05:29:31 - end all
	39	06:41:39 - 07:20:59	all	all	all	all
	40	07:37:23 - 08:17:19	all	all	all	all
25 July	41	08:19:29 - 08:53:09	all	all	07:37:27 - end	07:37:27 - end
	42	01:04:35 - 01:44:33	none	none	all	all
	43	02:17:04 - 02:57:02	none	none	none	none
	44	03:10:17 - 03:39:53	03:20:59 - end	03:20:55 - end	03:20:49 - end	03:20:33 - end
	45	03:48:09 - 03:58:29 04:00:11 - 04:40:09	03:48:17 - end all	03:48:29 - end all	03:48:13 - end all	03:48:13 - end all

Note: Frequency of target detection exceeded 95% for the time periods listed, except for those times marked by an asterisk (*), where the frequency was between 75% and 95%, or by double asterisks (**), where the frequency was less than 20%.

Table 1 (Concluded)

TIMES OF LIDAR DATA ACQUISITION AND TARGET DETECTION FOR 16 JULY AND 19-27 JULY

Date	Tape No.	Lidar Operation Times (EDT)	Times of Target Detection			10.6 μm
			0.53 μm	1.06 μm	3.8 μm	
26 July	46	04:41:53 - 04:48:41 05:19:39 - 05:26:29	all 05:19:47 - end	all 05:19:47 - end	all 05:19:43 - end	all 05:19:45 - end
	47	04:12:39 - 04:52:35	04:45:53 - end	none	none	04:44:27 - end
	48	04:58:02 - 05:38:00	all	all	all	all
	49	05:39:30 - 06:19:28	beg - 05:46:42 06:35:00-06:49:01**	beg - 05:45:46 none	beg - 05:45:38 none	beg - 05:46:40 06:34:54 - 06:49:01**
	50	06:21:10 - 07:01:09	07:09:35 - 07:12:53**	07:25:57 - end	07:27:21 - end	07:07:53 - 07:14:31
	51	07:02:45 - 07:42:43	07:24:43 - end			07:21:15 - 07:23:43*
27 July	52	00:02:32 - 00:42:32	none	none	none	07:23:55 - end
	53	00:44:06 - 00:51:47 01:45:34 - 02:01:56	none none	none none	none none	none none
		02:06:14 - 02:18:14	none	none	none	none
	54	19:04:46 - 19:44:41	19:04:54 - end	19:04:54 - end	19:04:50 - end	19:04:52 - end
	55	20:20:57 - 21:00:56	20:21:05 - end	20:21:05 - end	20:21:01 - end	20:21:03 - end
	56	21:02:46 - 21:42:44	beg - 21:10:12	beg - 21:09:40	beg - 21:09:54	beg - 21:10:08
	57	21:45:10 - 22:27:54	21:52:58 - end	21:52:54 - end	21:52:56 - end	21:52:56 - end
	58	22:39:04 - 22:43:20 22:44:52 - 23:22:02	22:39:12 - end all	22:39:08 - end all	22:39:10 - end all	22:39:10 - end all

Note: Frequency of target detection exceeded 95% for the time periods listed, except for those times marked by an asterisk (*), where the frequency was between 75% and 95%, or by double asterisks (**), where the frequency was less than 20%.

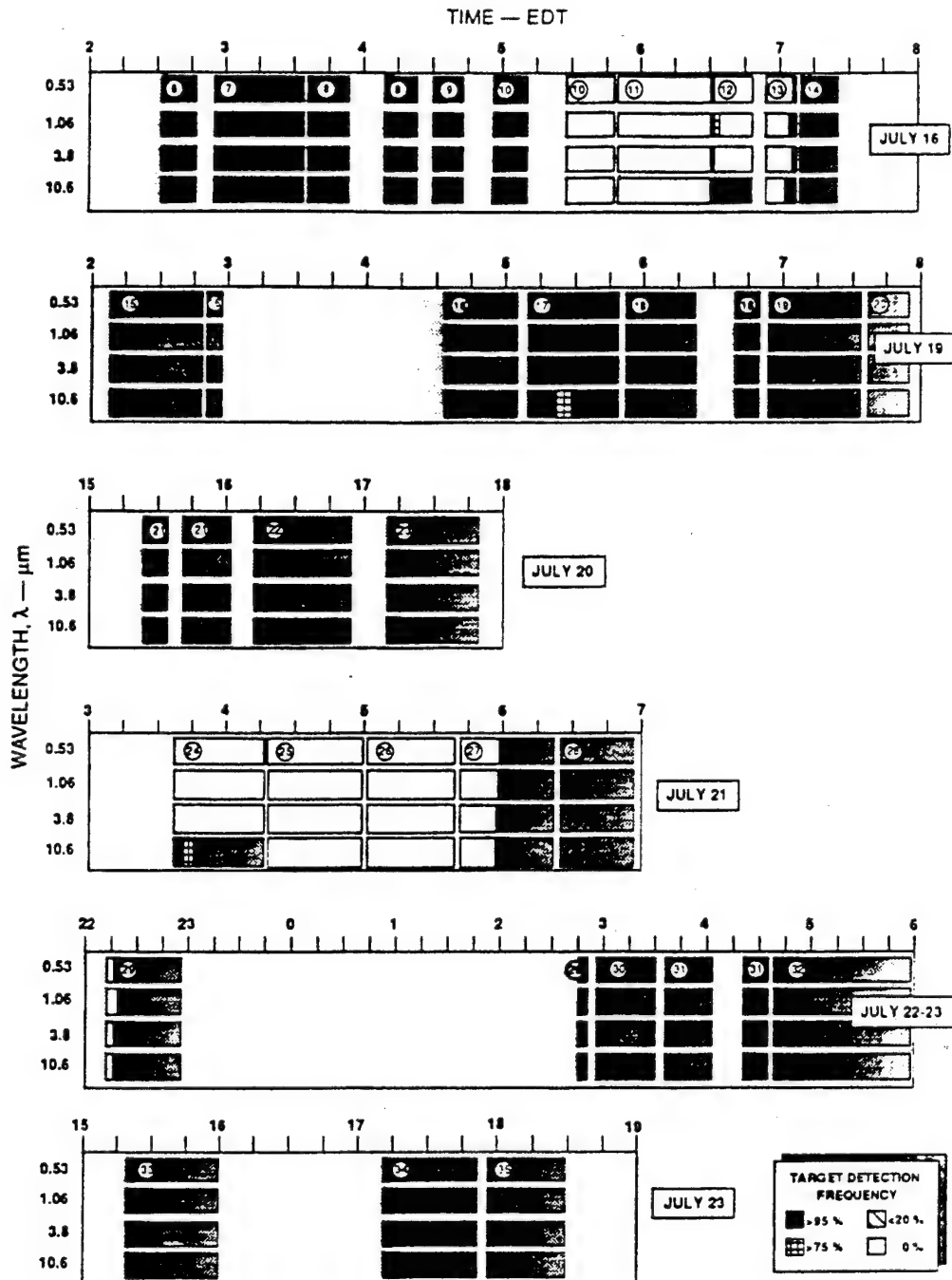


FIGURE 2 GRAPHIC DEPICTION OF TABLE 1 DATA

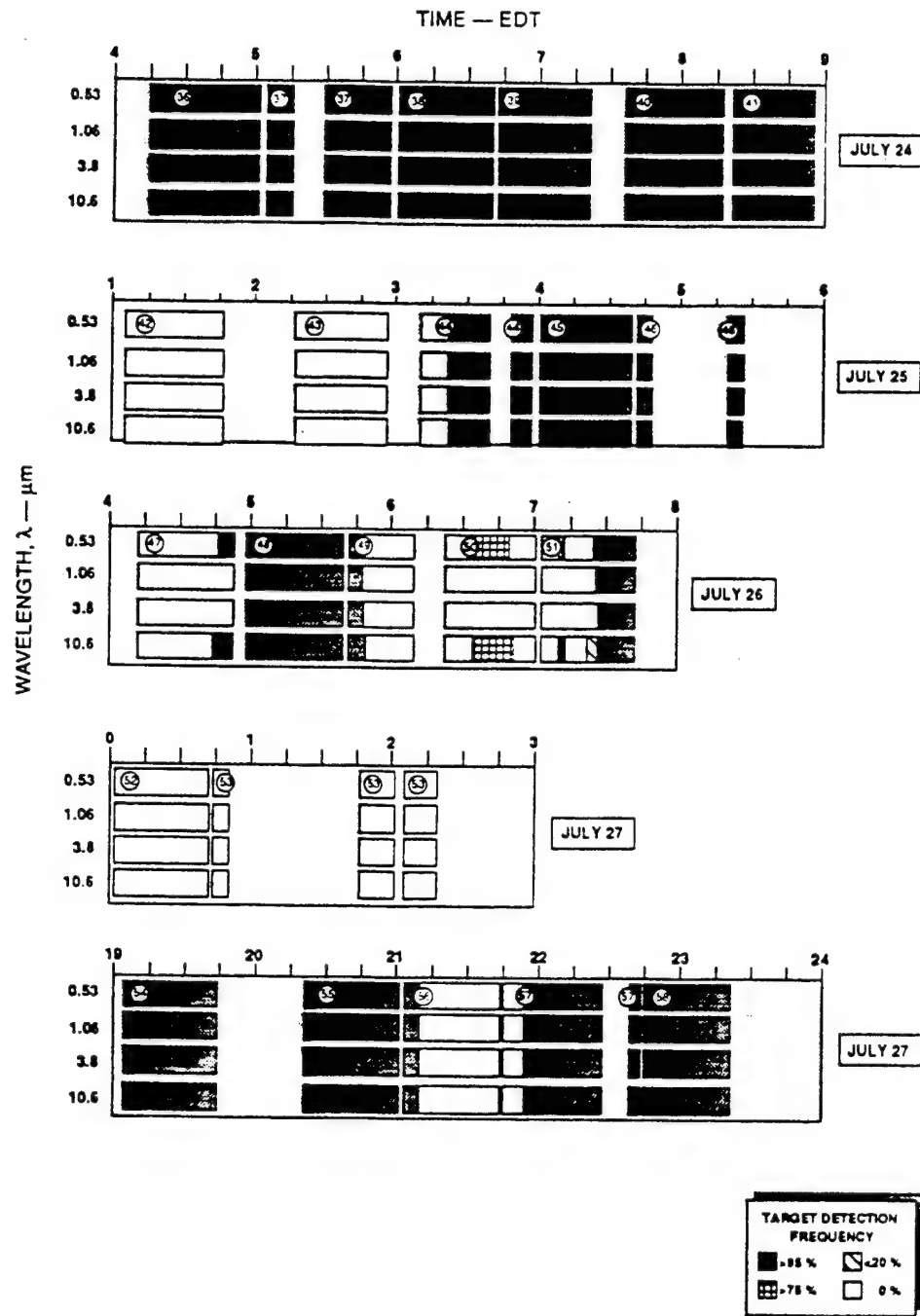


FIGURE 2 GRAPHIC DEPICTION OF TABLE 1 DATA (Concluded)

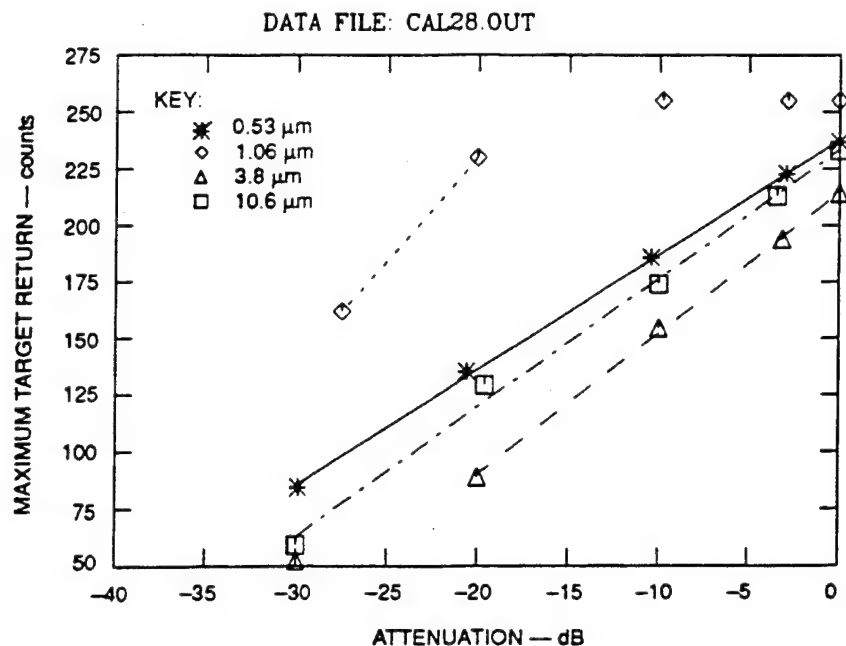


FIGURE 3 MEAN LIDAR TARGET RETURN MEASUREMENTS AND LEAST-SQUARES FITS FOR 21 JULY 1990

Table 2
SRI FLAPIR FOUR-WAVELENGTH LIDAR CALIBRATION RESULTS
(counts/dB)

Applicable Data Files	Wavelength (μm)				Calibration Runs Used
	0.53	1.06	3.8	10.6	
06 - 31	5.20 ± 0.09	9.15 ± 0.05	6.04 ± 0.15	5.56 ± 0.09	15, 22, 28, 29
32 - 46	5.09 ± 0.02	8.51 ± 0.04	$6.28 \pm .009$	5.50 ± 0.38	32, 41
47 - 58	4.50 ± 0.01	6.07 ± 0.09	4.26 ± 0.12	3.99 ± 0.01	54 (first), 58

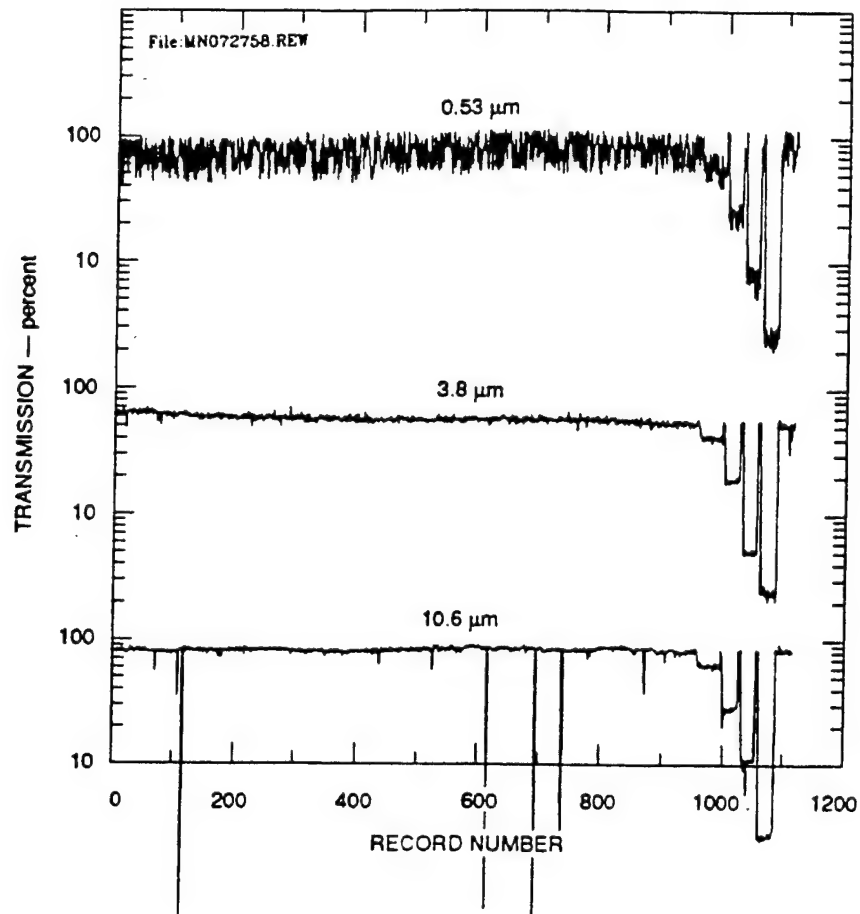
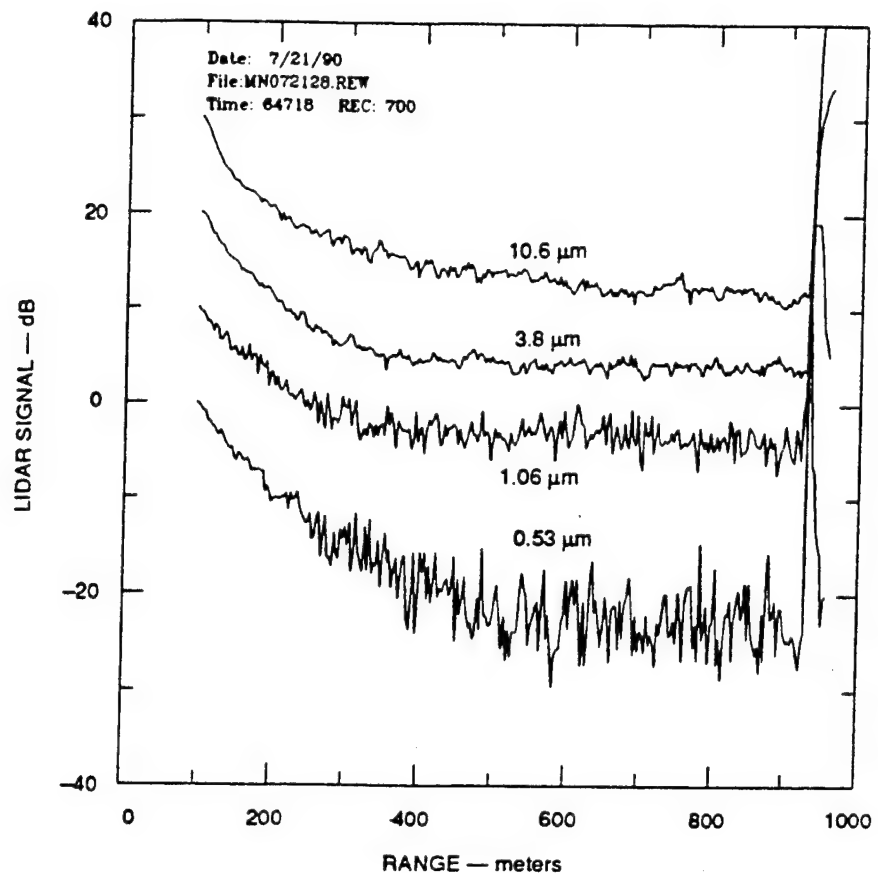


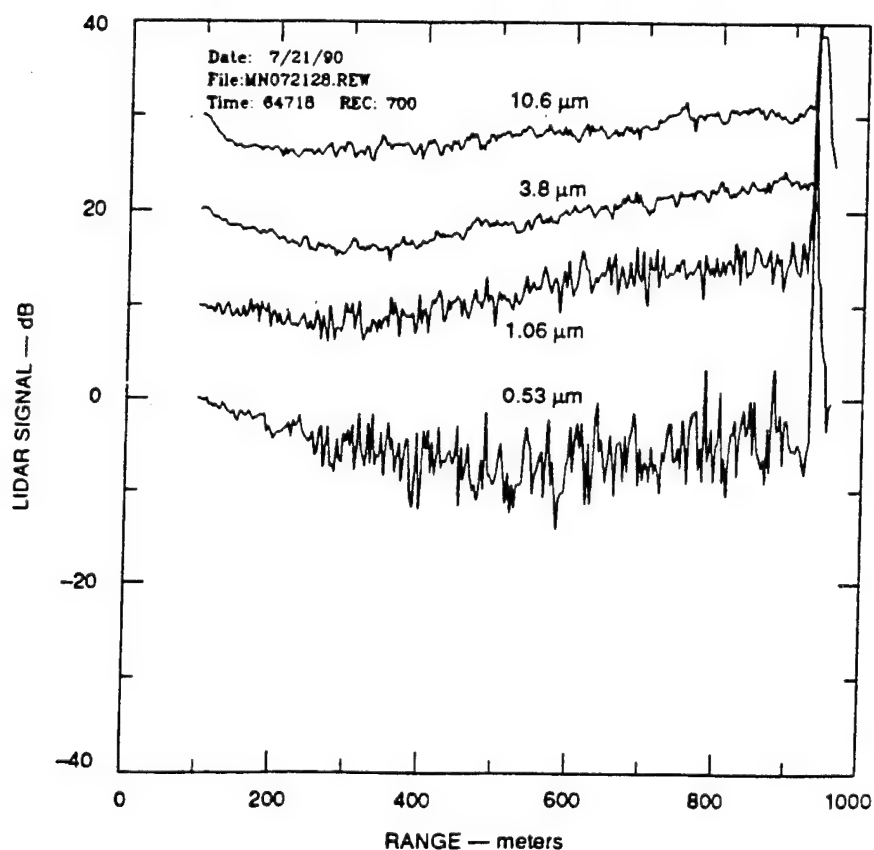
FIGURE 4 TARGET-DERIVED TRANSMISSION PERCENTAGES FOR 2244-2322 EDT, 27 JULY 1990

E. RANGE-RESOLVED BACKSCATTER RETURNS

The utility of the data set for calculating range-resolved backscatter values was investigated briefly. Several examples of range-resolved backscatter signatures were forwarded to Col. Koenig in a letter on 19 November 1991. Some of these are reproduced in this report. Figure 5(a) is an example of range-resolved lidar backscatter signatures (in dB) at the four wavelengths for a single shot along a relatively clear path on 21 July. The data have not been corrected for the range-squared dependence of the return signals. Figure 5(b) displays the same data with the geometric range dependence removed. The increase in signal with range beyond about 350 m at the three longest wavelengths indicates that the signal has fallen below the level of sensitivity of the system at those wavelengths; these data are not valid. (System sensitivity was substantially reduced to observe backscatter during fog conditions, and this explains why the



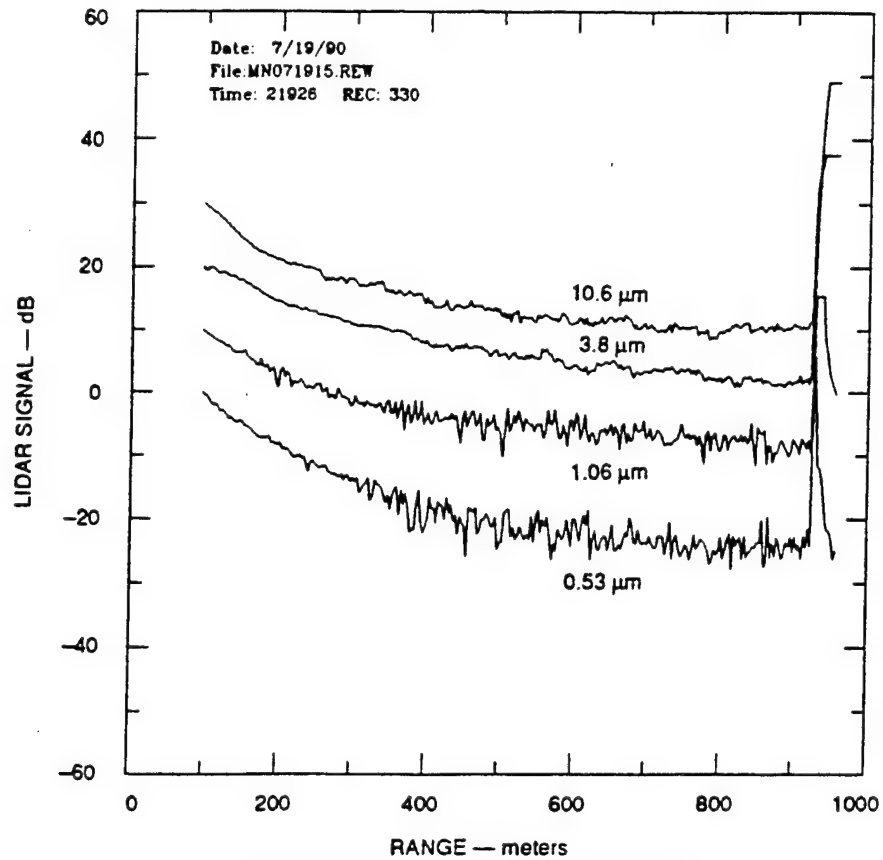
(a) BEFORE RANGE-SQUARED CORRECTION



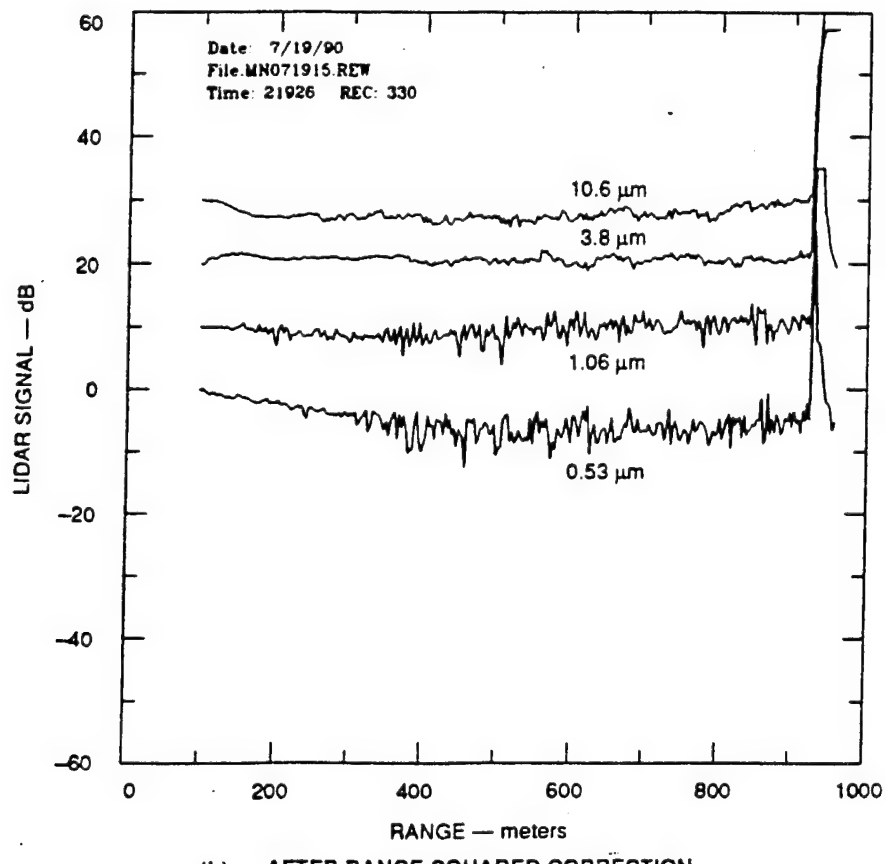
(b) AFTER RANGE-SQUARED CORRECTION

FIGURE 5 LIDAR RANGE-RESOLVED RELATIVE BACKSCATTER SIGNATURES
FOR 0647:18 EDT, 21 JULY 1990

lidar is able to observe backscatter only for short ranges during clear-air conditions.) Figure 6 shows analogous plots for a lidar record measured under fog-free, but somewhat hazy conditions on 19 July. The relative backscatter signatures indicate that the atmospheric extinction was too small to be evaluated at other than the $0.53\text{-}\mu\text{m}$ wavelength. Figure 7 shows the relative backscatter returns after the range-squared correction for a relatively foggy condition on 16 July. The data reflect large variations in fog density along the path; therefore, it may be difficult to correlate path-averaged data with *in-situ* data. However, there does appear to be a high degree of correlation among the range-resolved data at the various wavelengths. Also, the averaging effects of the longer pulse lengths at $10.6\text{ }\mu\text{m}$ and $3.8\text{ }\mu\text{m}$ are evident. Finally, Figure 7 illustrates one of the primary difficulties in deriving range-resolved optical parameters from the data, namely, difficulty in aligning the range scale of the backscatter returns at the various wavelengths. This problem is discussed in more detail in Section V.



(a) BEFORE RANGE-SQUARED CORRECTION



(b) AFTER RANGE-SQUARED CORRECTION

FIGURE 6 LIDAR RANGE-RESOLVED RELATIVE BACKSCATTER SIGNATURES

FOR 0219:26 EDT, 19 JULY 1990

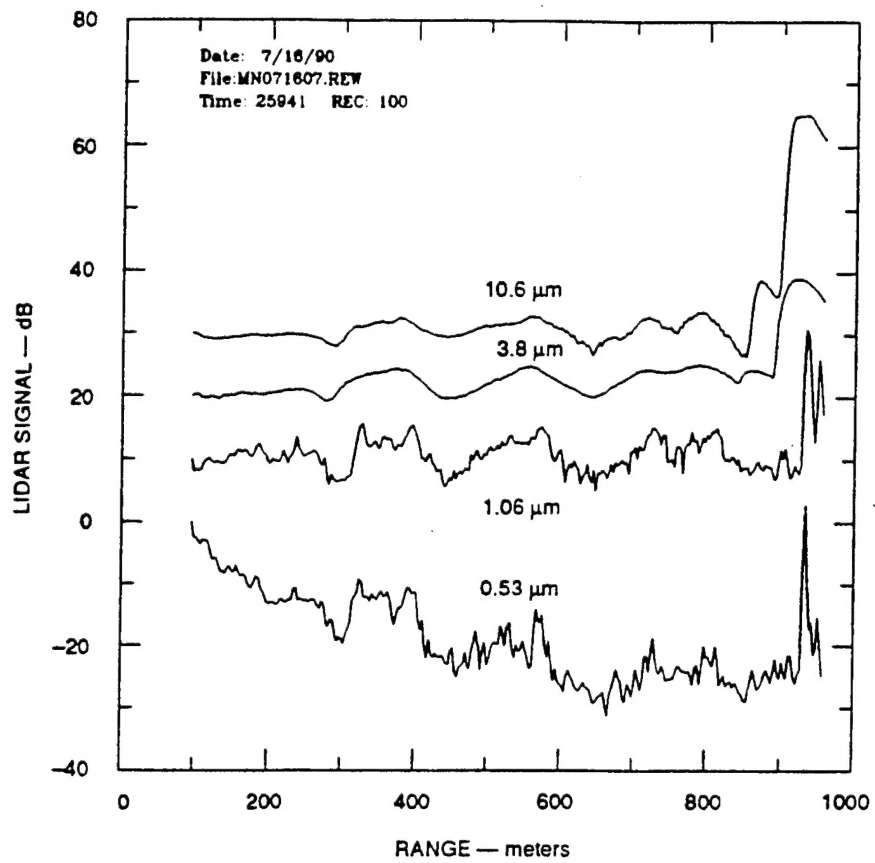


FIGURE 7 LIDAR RANGE-RESOLVED RELATIVE BACKSCATTER SIGNATURES FOR 0259:41 EDT, 16 JULY 1990, AFTER RANGE-SQUARED CORRECTION

5. DISCUSSION AND RECOMMENDATIONS

A number of issues were identified in analyzing the lidar data set collected during FLAPIR. These were detailed in the November 1991 letter to Col. Koenig. These considerations and others are summarized below:

Variability In Background Atmospheric Conditions Between and Within

Tests—Calculation of reliable path transmission values using the target method requires an accurate knowledge of the signals backscattered from the target under clear atmospheric conditions. Clear-air backscatter returns from the target were not always readily available before or after the FLAPIR runs, owing to changing atmospheric conditions. Hence, the clear-air target returns were generally assumed equal to the 0-dB intercept value derived from the least-squares fits of the target return data acquired during the calibration time periods when neutral-density filters were inserted into the receiver optical path. This assumption can lead to large biases in the target-derived transmissions if the assumed clear-air target return is incorrect by only a few counts, and could explain any gross discrepancies (biases) between SRI lidar-derived path transmissions and those reported by other investigators using other instruments.

Possible Variability of the Reflectance of the Target Due to Changing Weather Conditions—Target-derived transmission values could vary significantly if the reflectance of the target exhibited a strong dependence on its state of dryness/wetness, which is determined by atmospheric conditions. No quantification of this effectivity was attempted during FLAPIR.

Variability of Transmitted Laser Pulse Length Among Wavelengths and Between Lidar Shots—This affects the peak power transmitted by the laser and therefore introduces uncertainties in the target returns. Backscatter smoothing effects of the longer pulse lengths of the 3.8- and 10.6- μm lidar signatures relative to the 0.53- and 1.06- μm lidar signatures are obvious on the data plots of Figures 5 through 7.

Alignment of the Multiwavelength Signals with Respect to Range—This can be difficult under some atmospheric conditions when calculating and comparing range-resolved backscatter signatures. The backscatter signatures were aligned by first identifying the location of the target returns within the backscatter signal array. This was done by searching (separately for the range-resolved backscattered returns at each wavelength) for the maximum backscattered signal within a predefined range (i.e., in the vicinity of the target) for each shot. The multiwavelength backscatter signatures were then aligned either by aligning the maximum target returns for each wavelength or by searching backward (for each wavelength) toward the laser for the point where the slope of the backscatter trace begins to increase significantly toward the maximum target return and aligning the traces on this point. However, neither of these methods successfully aligned the backscatter signatures all the time because of varying laser pulse widths. Under relatively clear air conditions, the maximum target returns are of large amplitude and easy to

identify. However, the identification process becomes problematic as the atmospheric attenuation increases to the point that the maximum target amplitude becomes comparable to the noise in the signal.

Large Dynamic Range of Atmospheric Backscatter Values, and Limited Dynamic Range of Logarithmic Amplifiers—The 1.06- μm wavelength channel posed the biggest problem. Because of its high sensitivity (large number of ADC counts for 1 dB of attenuation), it was necessary to attenuate the 1.06- μm laser signal by about 30 dB during the data acquisition to keep the 1.06- μm target signal from saturating while at the same time being able to retain sensitivity to the atmospheric backscatter. Even so, subsequent calibration showed that the target returns remained saturated until an additional 20-dB optical filter was inserted in the optical path. As a result, at the 1.06- μm wavelength only, it was not possible to derive path transmission values using the target method whenever the one-way transmission exceeded about 10%.

Lack of Information on Transmitted Laser Energy—The laser energy monitors did not function properly during the trial; hence, no such data are available. This negates the ability to normalize out shot-to-shot energy variations and complicates analyses of temporal backscatter fluctuations. However, the laser energy variations are normally within 10 percent and should not greatly effect derived transmission histories.

SRI recommends that these effects be taken into account in performing additional analyses of the SRI FLAPIR lidar data.

6. ADMINISTRATIVE INFORMATION

A. CONTRIBUTORS

The following SRI scientists and engineers contributed to the research reported in this report:

- John M. Livingston, Senior Research Meteorologist
- Edward E. Uthe, Program Director, Atmospheric Science and Effects
- Norm B. Nielsen, Senior Research Engineer.

B. RELATED EFFORTS

No publications or articles resulted from total or partial sponsorship of the contract.